ACS OMEGA

http://pubs.acs.org/journal/acsodf

Article

Development of Quaternized Chitosan Integrated with Nanofibrous Polyacrylonitrile Mat as an Anion-Exchange Membrane

Aktilek Akhmetova, Bauyrzhan Myrzakhmetov, Yanwei Wang, Zhumabay Bakenov, and Almagul Mentbayeva*

Cite This: *ACS Omega* 2022, 7, 45371−45380

Read Online

ACCESS | Metrics & More | Article Recommendations | Supporting Information

ABSTRACT: A two-phase anion-exchange membrane was prepared from quaternized chitosan (QCS) integrated with an electrospun polyacrylonitrile (PAN) scaffold by spin coating. To synthesize QCS, glycidyltrimethylammonium chloride in various amounts was introduced into the structure of CS. The characterization of the cast cross-linked QCS (CQCS) membranes by impedance spectroscopy revealed the ionic conductivity (IC) in the range of 2.8×10^{-4} to 8.2×10^{-4} S cm^{-1} and the degree of quaternization (DQ) of 26.4−51.0%, where the CQCS film with the DQ of 51.0% showed excellent performance. When CQCS was reinforced with a PAN fiber mat, the newly developed composite membrane demonstrated the highest IC of 34×10^{-4} S cm^{-1} at 80 °C, low swelling, and an almost eightfold increase in tensile strength at a fully hydrated state compared to pristine materials. Moreover, the CQCS/PAN membrane was chemically stable and revealed increasing hydroxide transport during 1 month immersion in alkaline media.

1. INTRODUCTION

The growing demand for efficient green energy generation and storage systems has prompted the development of electrochemical devices such as fuel cells (FCs). Among all FC types, proton-exchange membrane fuel cells (PEMFCs) are the most mature and widely used ones owing to their high energy conversion efficiency, quick start-up, and availability of the proton-conducting membranes, including commercial ones such as Nafion and Aquivion with excellent tensile strength, chemical and thermal resistance, and high ionic conductivity.[1] The overall system is quite durable with a stable power output.[2] Nevertheless, some features of PEMFC's performance hamper its vast application. The limited choice of fuels,[2] the cost of poison-resistant and stainless noble metal catalysts to stimulate electrochemical reactions, and the preservation of stable performance at low pH are among the main issues.[3,4] Observing such drawbacks, the attention was shifted to fuel cells that could function in alkaline conditions−alkaline fuel cells (AFCs). The AFC can be a reasonable alternative to PEMFCs as it works in the same temperature range and consumes hydrogen gas as a fuel. Thus, owing to the different ion transport mechanisms of AFCs, more cost-effective transition-metal catalysts can facilitate their operation compared to the precious metals of the proton-exchange system.[4] Other advantages include faster oxygen reduction kinetics, enhanced cell voltage, and the use of a wider variety of fuels.[2,5]

Commonly, AFCs utilize potassium hydroxide (KOH) solution as an electrolyte; however, there are increased risks of leakage or electrode drying.[6,7] Besides, they readily react with CO_2, causing the formation of carbonates and simultaneously reducing the ionic conductivity and power output.[4,5,7] Considering these limitations, an alternative type of gel-like electrolyte, anion-exchange membrane (AEM), was introduced. Due to its polymer-based composition, CO_2 poisoning and leakages can be avoided.

For the successful commercialization and wide exploitation of AFCs, hydroxide-exchange polymer membranes should satisfy the following criteria:[2,7−9] reasonable OH^- conductivity with low location-based resistance, high current density operation, sufficient alkaline stability at elevated temperatures, full electron insulation, mechanical, thermal, and chemical stability, low cost, and abundance. Bae and others state that there is a trade-off in fulfilling all requirements.[9] For example, even though high ionic conductivity is the desired effect for the efficient work of FC, it might result in extensive water uptake and swelling ratio, leading to low mechanical stability.

Received: September 14, 2022
Accepted: November 17, 2022
Published: November 30, 2022

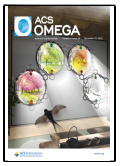

https://doi.org/10.1021/acsomega.2c05961
ACS Omega 2022, 7, 45371−45380

The selection of material for AEM plays a crucial role in the operation of AFC. So far, the preference for polymer backbone has been given to synthetic compounds, including polyketones, polyolefins, and polyethers.[10,11] In addition to synthetic materials, natural or naturally derived polymers such as chitosan (CS) and cellulose are captivating as they make the exploitation of fuel cells even more environment-friendly and cost-effective.[12−15]

CS is derived from chitin and consists of irregularly organized D-glucosamine and *N*-acetyl-D-glucosamine. This polysaccharide's structural arrangement and composition ensure its vast application as (1) an inhibitor of microbial growth in the food industry,[16,17] (2) a hydrogel for the removal of contaminants in wastewater remediation,[18] and (3) a biocompatible and mucoadhesive material in tissue engineering[18] and drug delivery,[19] respectively. Owing to its remarkable properties, chitosan has also been investigated as a polymer backbone of AEM because it is inexpensive and abundant. Also, it does not conduct electrons, which is one of the primary functions of the electrolytes in FCs.[14,20−22]

Nonetheless, the material's low anion conductivity and mechanical strength might hinder the AEM development. The scientific publications demonstrate the following ways of boosting the conductivity of CS:

- modifying D-glucosamine with cationic head groups such as quaternary ammonium ions;[21,23]
- inserting of fillers such as carbon nanotubes (CNTs),[24,25] silicon dioxide,[21] and quaternized halloysite nanotubes.;[26]
- blending CS with other polymers including poly(vinyl alcohol), poly(vinylidene fluoride), and poly(acrylic acid).[14,20,21,27]

While the OH conductivity of pristine CS membranes is ∼1 to 2 mS cm^{-1} at room temperature (RT),[26,28] it is almost two and six times higher in quaternary ammonium (QA)-grafted CS (QCS)[23,29] and QCS tuned with CNTs,[23] respectively. Despite increasing the ion transport capability, there is still room for the enhancement of the mechanical integrity of the hydrophilic chitosan material. Recently, Liu et al. developed QCS membranes reinforced with functionalized poly(vinylidene fluoride) nanofiber support for alkaline and acidic direct methanol fuel cells.[21,30] They achieved decent tensile strength (11.9 MPa) at a low swelling ratio (<50%) for QCS/QSiO2@PVDF compared to pristine QCS (220.5% and <1 MPa, respectively) upon total hydration of the membranes yet keeping the high ionic conductivity of ∼18 mS cm^{-1} of the composite AEM.[21]

To improve the tensile strength of the chitosan-based AEM, this paper focuses on (1) the structure and (2) the fabrication method of the membrane. The reliable structure was obtained through integrating QCS with a hydrophobic mechanical support−−electrospun polyacrylonitrile (PAN) yarns. The effectiveness of such membranes has already been justified in protein and water purification systems when cationic chitosan solution was cast on top of the PAN membrane.[31,32] However, to the best of our knowledge, a two-phase membrane composed of a QCS-coated PAN scaffold has not been utilized as an ion-exchange membrane for fuel cells yet. This study intends to show the applicability of the abovementioned structure and composition of the membrane for hydroxide transport and demonstrate its stability in alkaline conditions. To reach this goal, the current work modified the preparation method as well. Traditionally, a polymeric solution was combined with a nanofibrous scaffold by solution casting; however, this time, the spin-coating technique was utilized instead. The method enables homogenizing the surface and controlling the AEM's thickness, as the spin coater's parameters can adjust the QCS layer's thickness. Furthermore, the optimal DQ of the high-molecular-weight QCS was examined to maintain decent OH^- conduction.

2. MATERIALS AND METHODS

2.1. Materials. Chitosan (CS; degree of deacetylation = 90%, MW = 310,000−375,000), glycidyltrimethylammonium chloride (GTMAC), potassium hydroxide, and glass slides (22 mm × 22 mm) were purchased from Sigma Aldrich, Germany; polyacrylonitrile (PAN; MW = 150,000) was supplied by J&K Scientific, China. All reagents were used as received.

2.2. Characterization. *2.2.1. Physical and Chemical Properties.* The hydroxide conductivity of AEMs was evaluated by the electrochemical impedance spectroscopy method (Metrohm Autolab) scanned over the frequency range of 1 MHz to 1 Hz and the highest current of 100 mA. The surface morphology of the membranes was observed by a scanning electron microscope (Crossbeam 540 by Carl Zeiss) at a magnification of ×500 − ×10,000. The tensile parameters of films were tested by an electronic universal testing machine (WDW-3 by Jinan HST Group Co.). The quality of QA-functionalized CS synthesis was interpreted by a Nicolet iS10 Fourier transform infrared spectrometer (Thermo Fisher Scientific) at the wavenumber ranging from 4000 to 400 cm^{-1} with 32 scans per sample.

2.2.2. Degree of Quaternization. The Mohr titration of chloride ions with a standard silver nitrate solution is a common procedure used to define the content of QA-functionalized D-glucosamine in chitosan AEM.[24,33,34] In this work, conductometric titration was performed, where the standard 0.05 N silver nitrate solution was the titrant and 25 mL of 0.2 wt % synthesized QCS was the analyte. Once the equivalence of Ag^+ and Cl^- ions was established, the volume of $AgNO_3$ was recorded. The degree of quaternization (DQ) is given by:[35]

$$\mathrm{DQ} = \left\{\left[V_{\mathrm{AgNO_3}} \times \frac{c_{\mathrm{AgNO_3}}}{1000}\right]/[(V_{\mathrm{AgNO_3}} \times c_{\mathrm{AgNO_3}}/1000) + (m - (\mathrm{MW_2} \times V_{\mathrm{AgNO_3}} \times c_{\mathrm{AgNO_3}}/1000))/\mathrm{MW_1}]\right\} \times \frac{1}{\mathrm{DD}} \times 100\% \quad (1)$$

In eq 1, DD is the degree of deacetylation, MW_1 and MW_2 are the molecular weight (g/mol) of D-glucosamine and N-(2-hydroxyl) propyl-3-trimethyl ammonium chitosan chloride (HTCC), respectively, V_{AgNO_3} and c_{AgNO_3} are the volume (mL) and concentration (mol/L) of silver nitrate used for conductometric titration, and m is the mass (g) of HTCC dissolved in acid.

2.2.3. Water Uptake and Swelling Ratio. AEMs were cut in round disk shape (d = 18 mm) using a disc punching machine before testing and dried until constant weight. Then, they were placed in 1 M aqueous potassium hydroxide solution and deionized (DI) water for 24 h each. The weight and diameter in a fully hydrated state were measured. Water uptake (WU)

https://doi.org/10.1021/acsomega.2c05961
ACS Omega 2022, 7, 45371−45380

and swelling ratio (SR) were calculated by eqs 2 and 3, respectively:[36]

$$\mathrm{WU} = \frac{W_{\mathrm{wet}} - W_{\mathrm{dry}}}{W_{\mathrm{dry}}} \times 100\% \quad (2)$$

$$\mathrm{SR} = \frac{L_{\mathrm{wet}} - L_{\mathrm{dry}}}{L_{\mathrm{dry}}} \times 100\% \quad (3)$$

where W_{dry} and L_{dry} are the weight and length (diameter) of the dry membrane and W_{wet} and L_{wet} are the weight and length of the hydrated membrane, respectively.

2.2.4. Hydroxide Conductivity. The complete hydration of round-shaped membranes (d = 18 mm) was ensured by immersion in 1 M KOH and DI water for 24 h, respectively. The Nyquist plot of real versus imaginary impedance was used to calculate the membrane resistance. Then, the readings were inserted in eq 4, and the ionic conductivity (IC) value was determined[24]

$$\sigma = \frac{L}{R_{\mathrm{m}} S} \quad (4)$$

where σ is the ionic conductivity (S/cm), L is the distance between the electrodes (cm), R_{m} is the membrane resistance (Ω), S is the cross-sectional area of the membrane (cm^2), that is, S = width × thickness of the membrane.

2.2.5. Mechanical Properties. A tensile test was performed using an electronic universal testing machine (WDW-3 by Jinan HST Group Co.) to determine the mechanical properties of cast CS, PAN fibers, and composite membranes. The membranes were fully hydrated and cut into 2 × 5 cm with a clamping distance of 2 cm. The tensile test was performed at an elongation rate of 10 mm/min at room temperature and 1 atm. Then, the stress−strain curves were plotted.

2.3. Preparation of the CS Membrane and Synthesis of QCS. QCS was prepared according to the procedures used elsewhere.[34,37] CS powder (1 g) was dissolved in weak acetic acid (50 g, 2 wt %) to obtain a CS solution. GTMAC was added to the preheated CS solution in molar ratios of 2:1, 4:1, 6:1, 8:1, and 10:1 to the amino groups of CS in two portions. These products will be called QCS-2, QCS-4, QCS-6, QCS-8, and QCS-10, respectively. The mixture was stirred for 6 h at 80 °C and precipitated afterward in ethanol under vigorous stirring. The yellowish substance was washed twice as described above and dried overnight at 60 °C. The powdered QCS was dissolved in 2 wt % acetic acid and precipitated in ethanol one more time to remove the unreacted GTMAC. The purified substance was cross-linked by glutaraldehyde (GA), as reported in the literature.[38] A volume of 1.5 mL of 0.5 wt % GA was introduced dropwise in 15 g of 2 wt % QCS solution. Cross-linked QCS (CQCS) membranes were obtained by the solution casting method and dried at 60 °C until constant weight (see Table 1). Similarly, a cross-linked pristine CS (CCS) membrane was cast and used as a reference material.

2.4. Fabrication of PAN Fibers. The nanofiber mat was fabricated from the polymer solution by electrospinning (Ne200 NanoSpinner, Inovenso). PAN solution (8 wt %; dissolved in DMF) was sprayed, keeping the distance between the spraying nozzle and the glass film (collector) as 11 cm, and flow rate = 1 mL/h and voltage = 14 kV at room temperature.

2.5. Preparation of the Composite CQCS-10/PAN Membrane. PAN fibers on a glass slide were covered with a cross-linked QCS solution and allowed to impregnate for 1 h.

Table 1. Abbreviations of Cross-Linked Quaternized Chitosan Membranes

molar ratio of GTMAC to CS	name
0:1	CCS
2:1	CQCS-2
4:1	CQCS-4
6:1	CQCS-6
8:1	CQCS-8
10:1	CQCS-10

After that, the excess QCS was removed from the composite membrane by a spin coater (SPIN150i; Polos). The parameters are as follows: speed−−3000 rpm, acceleration−−500 rpm/s, and time of spinning−−300 s. Overall, four layers of QCS were formed by drying for 30 min to make a sheath of fibers.

3. RESULTS AND DISCUSSION

Chitosan can be readily modified cationically due to the availability of amine groups in its structure. One of the most promising ways of such functionalization is quaternary ammonium (QA) grafting with pyridinium, benzyltrimethylammonium, 1,4-diazabicyclo [2.2.2] octane, *n*-methyl piperidinium, guanidium, trimethylhexylammonium, and glycidyltrimethylammonium groups on CS polymers' backbone.[39,40] It was reported that glycidyltrimethylammonium chloride (GTMAC) shows excellent compatibility with the NH_2 groups of D-glucosamine by numerous studies.[34,41,42] The concentration of GTMAC shall be adapted for the molecular weight and degree of deacetylation (DD) of the current raw CS material. Thus, the molar ratio of GTMAC was varied with respect to D-glucosamine, as described in Materials and Methods. The introduction of positively charged groups increased the solubility of the chitosan films in water, making them more brittle in dry state. Therefore, the polymer chains of the synthesized QCS samples were cross-linked with the widely used cross-linking agent, glutaraldehyde (GA). After careful analysis, the appropriate concentration of GA was found to be 0.05 wt %, which was fixed to all cross-linked QCS (CQCS) membranes.

After preparing CQCS materials, several characterizations have been conducted to analyze the chemical stability in alkaline conditions and the OH^- transportation ability. The DQ analysis and FTIR spectra of all QA-incorporated chitosan membranes demonstrated whether the outcome of the synthesis was successful or not. The water uptake (WU) and swelling ratio (SR) tests evaluated the water content of QCS membranes, whereas the ionic conductivity (IC) test results revealed hydroxide-exchange properties. Based on those techniques, the optimal cationic chitosan material was selected for integration with the PAN support.

Figure 1 schematically illustrates the process of CQCS/PAN AEM fabrication. First, polyacrylonitrile fibers were formed using the electrospinning technique. The QCS solution was prepared and cross-linked with glutaraldehyde. Then, the CQCS solution was dropped on electrospun threads and uniformly distributed with the pores of the nanofiber mat using a spin coater. To ensure the denseness of the nanofibrous membrane, once the AEM was completely dried after the coating process, step 3 from Figure 1 was repeated three more times.

https://doi.org/10.1021/acsomega.2c05961
ACS Omega 2022, 7, 45371−45380

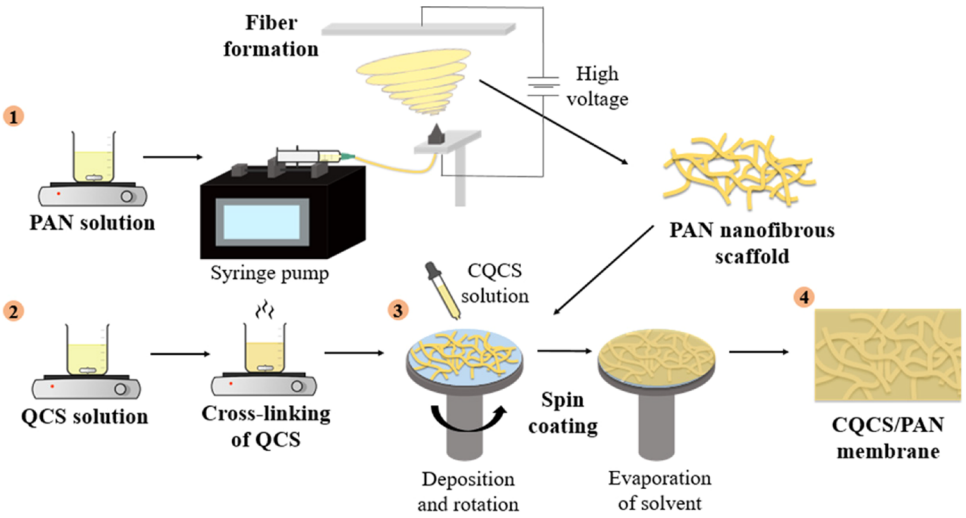

Figure 1. Schematic representation of the AEM fabrication.

3.1. Determination of the Degree of Quaternization of QCS. The WU, SR, and IC strongly depend on the DQ of chitosan, which expresses the quantity of positively charged QA groups in the polymer chain.[43] The DQ can be controlled by altering the temperature, reaction time, quaternizing agent concentration, and the medium's pH.[44] In addition, the increase in temperature helps to overcome the reaction barrier, and the quaternization of hydroxyl groups of chitosan at high pH is more favorable in terms of thermodynamics and kinetics.[45,46]

The DQ of all synthesized QCS materials was calculated using the conductometric titration method (see the Supporting Information). Indeed, the increase of GTMAC concentration contributed to higher DQ values, which were 26.4, 32.0, 38.1, 43.3, and 51.0% for QCS-2, QCS-4, QCS-6, QCS-8, and QCS-10, respectively.

3.2. FTIR Analysis of Pristine and Quaternized CS Membranes. Chitosan is a copolymer that has acetamide ($-NHCOCH_3$) and amino ($-NH_2$) groups. After the deacetylation of chitin under heterogeneous conditions, the intensity of the band absorption of amide-I (C═O stretching vibrations of secondary amide) decreases because of the conversion to amide-II (stretching vibrations of CN) with a lower frequency. Further, it transforms into the NH_2 group of the primary amine. The intensity of the amide-II band is stronger for chitosan, which has a higher degree of deacetylation.[47]

Figure 2 exhibits the FTIR spectra of chitosan and quaternized chitosan with different DQ values. The FTIR spectrum of chitosan shows the combined absorption bands of OH and NH, which are involved in hydrogen bonding in the wide bands in the region of 3600−3100 cm^{-1}, where bands at 3500−3300 cm^{-1} are assigned to the OH stretching and bands at 3360−3300 cm^{-1} are due to NH_2 stretching.[48] Furthermore, the absorption band at 2924 cm^{-1} is assigned to the asymmetric and symmetric C−H stretching of the CH_2 and CH_3 groups.[40] The existence of quaternary ammonium groups on the backbone of the polymer was confirmed by the appearance of a strong absorption band at 1480 cm^{-1}, which is due to the C−H bending of the trimethylammonium group of GTMAC.[42,49,50] This vibration band at 1480 cm^{-1} could be seen when the ratio of GTMAC/CS reached a value of 6:1 and then continued to increase proportionally.

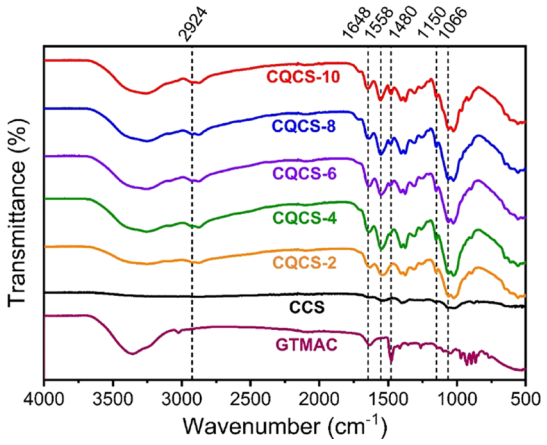

Figure 2. FTIR spectra of CCS and CQCS membranes.

Additionally, unchanged alcohol bands between 1150 and 1066 cm^{-1} indicated the quaternization of only the available NH_2 groups of CS by GTMAC. A band observed at 1648 cm^{-1} suggests the incomplete deacetylation of the amide-I group of chitin and cross-linking of quaternized chitosan membranes with glutaraldehyde. Namely, the presence of (C═N) imine bonds shows the successful cross-linking of membranes which can be detected between 1640 and 1570 cm^{-1}, overlapped with the −NH vibrations of original CS.[51]

3.3. WU and SR of Pristine and Quaternized CS Membranes. The ability of the material to interact with water is essential for completing AEM requirements. Generally, extremely high or low water content might result in inefficient performance, even though the conventional values of WU and SR differ in various membranes. When it comes to low water absorption, deficiency of hydroxide groups might occur. In the case of excessive hydrophilicity of AEM, the concentration of OH^- might drop due to the dilution effect.[20]

It is expected that the QA groups of QCS are hydrophilic, and they can lead to an increase in WU and SR. Consequently, the AEM's IC and mechanical properties can deteriorate due to the membrane's deformation and dimensional instability. However, the absorbed water molecules tend to hydrate hydroxide ions and support their transportation through the AEM. Therefore, WU should be carefully balanced in the

https://doi.org/10.1021/acsomega.2c05961
ACS Omega 2022, 7, 45371−45380

AEM. All these parameters can be improved by cross-linking the polymer or developing composite membranes.[52,53]

Figure 3 shows that the QA modification affected the WU and SR of membranes differently. As water absorption and

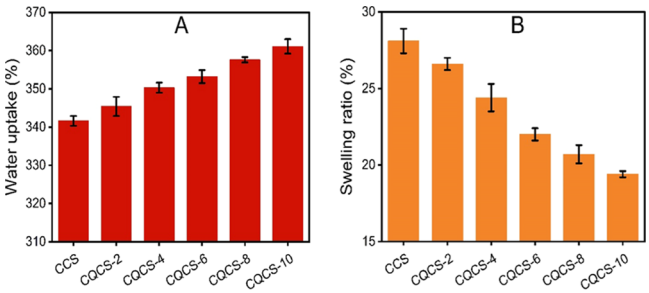

Figure 3. Water uptake (A) and swelling ratio (B) of cast membranes.

swelling are associated with cross-linking, these parameters were successfully controlled by reacting CS with GA.

As seen in Figure 3A, the lowest content of WU is observed for CCS, with a value of 341.6 ± 1.3%. As DQ rises from 26.4 to 51.0%, WU gradually increases due to the interaction of charged groups with water molecules. Yet, there is no crucial difference, and maximum uptake is around 360% for CQCS-10, which is favorable for mechanical stability. It was expected that SR would expand with the increasing WU of the membranes. However, the incorporation of QA groups on the polymer's backbone and cross-linking led to decreased swelling (see Figure 3B).[36,54] This could be a consequence of the physical attraction between the positively charged ammonium head and negatively charged groups of the membranes.

CQCS-10, with a DQ of 51.0%, has a limited amount of free amino groups, and during the cross-linking, 0.05 wt % GA reacts with the free amino groups of chitosan. As a result, hydrogen bonds between the amino groups and water molecules can be reduced due to the decrease in the membrane mobility by the interconnection of chains.[55] While CCS and other cast membranes with lower DQ have more free amino groups, the concentration of GA was insufficient for cross-linking, resulting in a more significant volume expansion. Therefore, due to the presence of more QA groups than in the other membranes, CQCS-10 has the highest WU and lowest SR without any deterioration of mechanical strength.

3.4. Hydroxide Conductivity of Pristine and Quaternized CS Membranes. Prior to testing the ionic conductivity, the pristine CQCS membranes were immersed in 1 M potassium hydroxide solution for 24 h and then in deionized water for the same period. All raw CQCS materials of various DQ values were tested by preparing cast membranes of thickness around 240 μm to observe the impact of quaternization on IC. Figure 4A summarizes the Nyquist plots of CCS and CQCS AEMs obtained by electrochemical impedance spectroscopy at the 1 MHz−1 Hz frequency range. The bulk resistance (R_m) of hydrated membranes was determined at the intercept of the semicircle with the real impedance axis. CQCS-10 revealed the smallest R_m and was expected to show a sufficient ion transfer. Figure 4B illustrates the hydroxide conductivities of pristine and modified CS membranes, which were measured at room temperature and ranged between 2.6×10^{-4} and 8.2×10^{-4} S cm^{-1}. Indeed, DQ

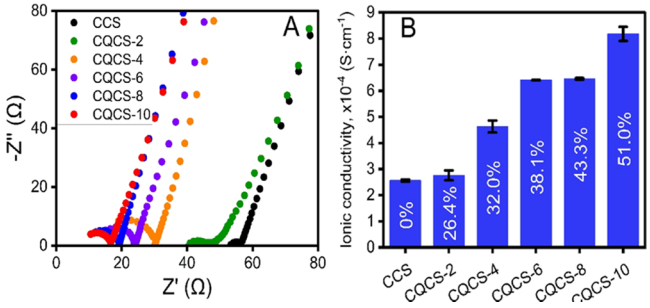

Figure 4. Ionic conductivity of cross-linked pristine and QA-grafted CS membranes measured at RT: (A) Nyquist plots and (B) IC versus corresponding DQ (shown as %).

directly impacts OH^- transport as quaternization dramatically boosts the ion conductivity of functionalized CS membranes compared to control CCS. Thus, ICs of CCS and QCS-2 AEMs reveal similar values, whereas the high content of QA groups in QCS-6, QCS-8, and QCS-10 results in a nearly two- to threefold increase.

The electrical equivalent circuit (EEC) model of the system of the studied membranes is shown in Figure 5. The EEC

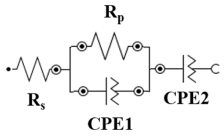

Figure 5. Model of an EEC of AEMs.

includes R_s (electrolyte resistance), R_p (polarization resistance), and two constant phase elements (CPE). R_s, R_p, and CPE1 appear in the high-frequency region as a semicircle, in which R_p and CPE1 are connected in parallel and characterize membrane conduction properties. The low-frequency straight line CPE2 indicates the electrical double-layer capacitance (EDCL) with a phase of $(-90 \times n)°$. The characteristic parameter n values of CPE1 and CPE2 were 0.838 and 0.828, respectively. It means that CPE1 with a value of n = 0.838 showed an imperfect semicircle, and CPE2 with a value of n = 0.828 describes more capacitor behavior than resistor due to the roughness of the membrane/electrode border or EDCL at the blocking electrodes. As a result of fitting and drawing the EEC, the estimated errors of R_s, R_p, and n were observed to be 4.7, 3.9, and 0.3%, respectively.

3.5. Characterization of the Composite CQCS-10/PAN Membrane. CQCS materials with different DQ values were carefully investigated based on the water-absorbing and ion-conductive properties. QCS-6, QCS-8, and QCS-10 revealed QA grafting accomplished in the FTIR spectrum. CQCS-10 exhibited the highest DQ and OH^- conduction, sufficient hydration, and cross-linking among these three samples. Therefore, it was selected to fabricate a composite membrane with a PAN fiber network.

3.5.1. FTIR of Pristine Materials and the Composite Membrane. After the integration of the two phases, the presence of the incorporated cationic head groups in QCS and proper interactions between PAN and QCS were studied by FTIR. The IR spectra of electrospun PAN fibers, CQCS-10, and the spin-coated CQCS-10/PAN membrane are shown in Figure 6. The bands at 2924 and 1450 cm^{-1} are ascribed to the symmetrical stretching vibration and symmetrical bending

https://doi.org/10.1021/acsomega.2c05961
ACS Omega 2022, 7, 45371−45380

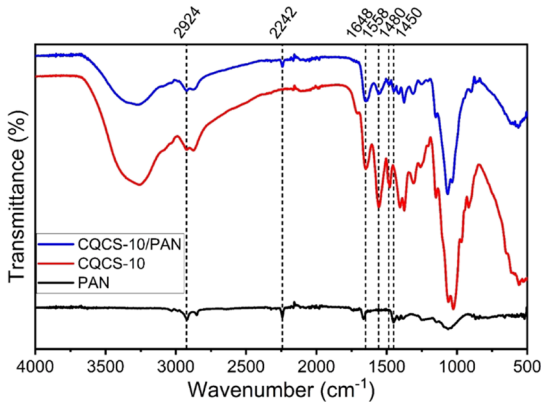

Figure 6. FTIR spectra of PAN, CQCS, and CQCS-10/PAN composite membrane.

vibration of C−H (υ_s(C−H) and δ_s(C−H) in CH_2), respectively. The formation of [−HC−N═N−CH−] conjugation indicates the cross-linking of PAN fibers which vibrates at 1664 cm^{-1}.[56] The band at 2242 cm^{-1} corresponds to the stretching vibration of the nitrile group $\upsilon_{C\equiv N}$.[57] In a composite membrane of CQCS-10/PAN, the intensity of the band at 1558 cm^{-1} reduced, while the intensity at 1648 cm^{-1} increased, which shows the overlapping of C−O (amide-I) of CS and C−N of PAN. Furthermore, the intensity of bands at 1450 and 1480 cm^{-1} in the CQCS-10/PAN membrane reduced. It might be due to the interaction between the CH_2 bending of PAN and the $-CH_3$ bending vibrations of GTMAC in the chitosan backbone. According to the FTIR results, chemical interactions between PAN and CQCS are apparent, which could improve the mechanical properties of composite membranes.[58]

3.5.2. Surface Characterization of Pristine PAN Fibers and the CQCS-10/PAN Composite Membrane. The surface morphologies of pristine PAN nanofibers and CQCS reinforced with PAN yarn mat are observed by SEM and illustrated in Figure 7. Electrospun PAN nanofibers were randomly arranged, and the diameter may have appeared in different sizes. The shape and surface of the fibers were straight and smooth, respectively. The fibers had a large surface area, and no beads were observed (Figure 7A). Impregnation of PAN fibers with another polymer filled the voids between them and was expected to form a more durable and rigid material (see Figure 7B).

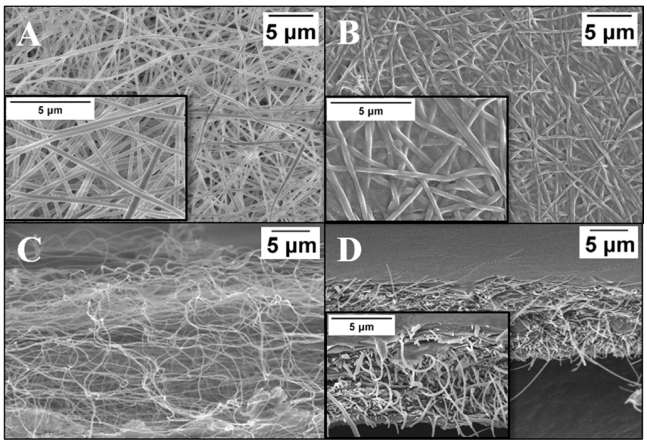

Figure 7. Scanning electron micrographs of the top (A) and cross-sectional (C) views of PAN fibers and the corresponding images (B, D) of the CQCS-10/PAN membrane.

The SEM images of the cross sections of pristine PAN threads and the composite membrane were obtained to assess the ability of the depositing CQCS solution to penetrate all the sublayers of the fiber mat. From Figure 7C,D, one can observe that the blank spaces between yarns were occupied by QA chitosan.

3.5.3. Water Content and Hydroxide Conductivity Tests of a Composite Membrane. The long-term performance of alkaline fuel cells highly depends on the dimensional stability that can be improved by controlling WU and SR.[24,54] To fulfill this requirement, WU and SR of the obtained composite CQCS-10/PAN membranes were measured. The fibers significantly restricted the hydration of the CQCS-10/PAN membrane compared to pure CQCS membranes. For instance, the WU and SR values of the latter were more than 300 and 20%, respectively, while the composite PAN-based membranes exhibited WU of only 124.0 ± 5.5% and SR of 1.7 ± 0.1% (see Table 2).

Table 2. Water Content and Ionic Conductivity Data of the Pristine and PAN-Reinforced CQCS Membrane

AEM type	SR ± STD, %	WU ± STD, %	IC ± STD ($\delta \times 10^{-4}$ S cm^{-1})
CQCS-10/PAN	1.7 ± 0.1	124.0 ± 5.5	6.7 ± 0.3
CQCS-10	19.4 ± 0.2	361.1 ± 1.9	8.2 ± 0.3

The preservation of electrochemical properties of CQCS-10 after the insertion of a thread mat was examined and compared to the pristine cationic material. The δ value of the composite QCS-10-coated PAN membrane (6.7×10^{-4} S cm^{-1}) was comparable but slightly lower than that of QCS-10. This phenomenon is frequently met when the properties of chitosan are tuned with additional materials. In this work, the presence of PAN having its own resistivity decreases the overall IC. Another study investigated cast CNT-functionalized QCS membranes that had a slight drop in conductivity due to the anions' restricted conduction path after the fillers' introduction.[24] Liu et al. fabricated an AEM of a similar fabrication technique and structure to ours, namely QCS-coated PVDF fiber film.[21] When they compared the electrochemical performance of the composite membrane with the pristine QCS, it was twice less conductive. Thus, some trade-off between the mechanical and ion-conductive properties is tolerable for maintaining the physical integrity of the AEM.

3.5.4. Mechanical Properties of Pristine Materials and the Composite Membrane. The stress−strain curves in Figure 8A present the response of the cross-linked materials to applied stress. Cross-linking is expected to decrease membrane deformation; thus, it might lose the elastic properties and become more brittle.[55] The high DoD (90%) of the CS material grants numerous NH_2 groups for reactions with quaternizing and cross-linking agents. CQCS-10, with a DQ of 51.0%, had the highest WU among all CS membranes, making it more hydrophilic and, thus, mechanically weaker at a fully hydrated state. The tensile strength and breaking strain of CQCS-10 were 0.1 MPa and 0.49%, respectively, which were only ∼1.3 times lower than those of unmodified CS film.

The alternative behavior of PAN yarn-based membranes is observed in Figure 8B. Namely, PAN and CQCS-10/PAN

https://doi.org/10.1021/acsomega.2c05961
ACS Omega 2022, 7, 45371−45380

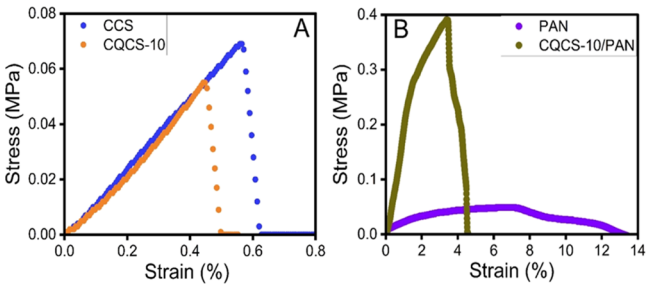

Figure 8. Stress−strain curves of (A) cast pristine and modified chitosan and (B) PAN fiber network and composite CQCS-10/PAN.

were more resilient, and they did not tear readily but preserved their integrity by rupturing gradually. As these films undergo alkaline treatment, partial hydrolysis might occur, and some nitrile groups of PAN could be converted to carboxylate groups.[59] This process facilitates the formation of additional electrostatic forces (e.g., hydrogen bonds) within PAN and between QCS-10 and PAN. The Control PAN fiber mat showed breaking stress comparable to the cast chitosan membranes with strength under 0.1 MPa and elongation at a break of 13.2%. The tensile strength of CQCS-integrated PAN revealed a nearly eightfold increase, whereas the strain was 3.4%. This behavior might be reasonable as the coating of fibers and voids restricted the mobility of PAN polymer chains with chitosan.

The mechanical properties of these films would probably be even higher if they were thicker. However, to satisfy the requirements of an AEM, the membranes were thin. Overall, developing a two-phase AEM improved the mechanical properties of pristine materials; namely, it possessed greater elasticity than CS and higher stress resistance than CS and PAN, respectively.

3.5.5. Chemical Stability of the Composite Membrane. As discussed above, alkaline media can positively affect the cohesion of QCS and PAN due to the hydrolysis of PAN and the establishment of electrostatic attraction. Additionally, the basic treatment hinders the excessive deformations of chitosan as it neutralizes residual acetic acid in the membrane.[55] Thus, KOH can reinforce the composite CQCS-10/PAN membrane along with cross-linking with glutaraldehyde. To confirm their chemical stability, the films were immersed in 1 M KOH for 30 days at room temperature, and IC was measured every 3 days. Figure 9A illustrates the Nyquist plots of the EIS measurements, revealing the reduction of membrane resistance with the increased immersion time.

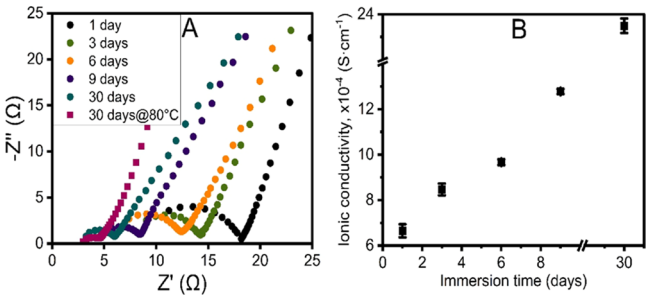

Figure 9. Ionic conductivity of the composite CQCS-10/PAN membrane immersed in 1 M KOH for 1−30 days and measured at RT: (A) Nyquist plots and (B) IC vs time.

Consequently, the ionic conductivity of CQCS-10/PAN membranes is inversely proportional to R_m. The expanded surface area of the yarn-based membrane and the presence of hollow spaces in its structure allowed sufficient QCS-based coating that created more paths to transport OH^- ions. The anion conductivity of the composite membrane rises gradually, reaching the highest value of 1.3 mS cm^{-1} on the ninth day (see Figure 9B). This trend is observed even after 30 days of storing the composite AEM in the alkaline solution, as the δ value elevated to 2.4 mS cm^{-1} at RT. The ionic conductivity was measured at 80 °C to monitor the thermal effect on the hydroxide-transport ability of the membrane. Commonly, elevated temperature stimulates faster ion transfer, thus boosting anion conductivity.[60] Indeed, the maximum IC of 3.4 mS cm^{-1} was reached. At the same time, the immersion of CQCS-10/PAN membranes into 1 M KOH for 30 days did not affect the mechanical strength significantly. It is the partial hydrolysis of PAN threads and consequent strengthening of the membranes, as discussed in the work of Jin et al.,[61] that are mainly responsible for the mechanical durability of the composite membrane.

As the ionic conductivity increased over the time of immersion in alkaline solution, the degradation of material was probably negligible. Thus, the degree of QCS's cross-linking and compatibility with the PAN fiber mat was enough to preserve the AEM's durability and simultaneously exhibit decent IC.

4. CONCLUSIONS

This work demonstrates the fabrication of a rigid anion-exchange membrane comprising a cationically functionalized chitosan polymer reinforced with a PAN nanofiber network. During the synthesis of QCS, the variation of the GTMAC concentration enabled the selection of optimal DQ (51.0%) that made the material hydrophilic yet stable upon cross-linking. The impregnation of PAN threads via the spin-coating technique made the distribution of CQCS uniform within the pores. Upon tensile testing, the strength of the composite membrane was ∼7 times higher than that of the cast CQCS-10 film, which shows that fibers had been the main contributors to the mechanical toughness of CQCS-10/PAN. This scaffold integration did not affect IC significantly as it was comparable to control CQCS-10 when immersed in an alkaline solution for 24 h at room temperature. Indeed, the increase of OH^- conductivity after 30 days was almost fourfold at RT and around fivefold at 80 °C. Thus, the composite CQCS-10-coated PAN AEM can fulfill the requirement of being ion-conductive and mechanically and chemically stable AEM.

■ ASSOCIATED CONTENT

Supporting Information

The Supporting Information is available free of charge at https://pubs.acs.org/doi/10.1021/acsomega.2c05961.

Conductometric titration plots of QCS-10 and pristine CS (PDF)

■ AUTHOR INFORMATION

Corresponding Author

Almagul Mentbayeva − *Department of Chemical and Materials Engineering, School of Engineering and Digital Sciences, Nazarbayev University, Nur-Sultan 010000,*

https://doi.org/10.1021/acsomega.2c05961
ACS Omega 2022, 7, 45371−45380

Kazakhstan; orcid.org/0000-0001-9132-1173; Email: almagul.mentbayeva@nu.edu.kz

Authors

Aktilek Akhmetova − *Department of Chemical and Materials Engineering, School of Engineering and Digital Sciences, Nazarbayev University, Nur-Sultan 010000, Kazakhstan;* orcid.org/0000-0001-7838-3513

Bauyrzhan Myrzakhmetov − *Center for Energy and Advanced Materials Science, National Laboratory Astana, Nazarbayev University, Nur-Sultan 010000, Kazakhstan*

Yanwei Wang − *Department of Chemical and Materials Engineering, School of Engineering and Digital Sciences, Nazarbayev University, Nur-Sultan 010000, Kazakhstan; Center for Energy and Advanced Materials Science, National Laboratory Astana, Nazarbayev University, Nur-Sultan 010000, Kazakhstan;* orcid.org/0000-0002-8488-9833

Zhumabay Bakenov − *Department of Chemical and Materials Engineering, School of Engineering and Digital Sciences, Nazarbayev University, Nur-Sultan 010000, Kazakhstan; Center for Energy and Advanced Materials Science, National Laboratory Astana, Nazarbayev University, Nur-Sultan 010000, Kazakhstan;* orcid.org/0000-0003-2781-4955

Complete contact information is available at: https://pubs.acs.org/10.1021/acsomega.2c05961

Author Contributions

A.A.: Conceptualization, investigation, methodology, data curation, writing−−original draft, and writing−−review and editing. B.M.: Conceptualization, investigation, methodology, data curation, and writing−−original draft. Y.W.: Supervision, conceptualization, funding acquisition, validation, and writing−−review and editing. Z.B.: Supervision, funding acquisition, and validation. A.M.: Supervision, project administration, conceptualization, funding acquisition, validation, and writing−−review and editing.

Notes

The authors declare no competing financial interest.

■ ACKNOWLEDGMENTS

This work was supported by the research grants AP09057868 for "High performance polymer-based anion-exchange membranes for alkaline fuel cells" project from MES RK and 080420FD1906 for "Development of composite anion-exchange membranes with improved chemical and mechanical stability" from Nazarbayev University.

■ REFERENCES

(1) Zhang, J.; Zhang, H.; Wu, J.; Zhang, J.Chapter 1 - PEM Fuel Cell Fundamentals; Zhang, J., Zhang, H., Wu, J., Zhang, J., Eds.; Elsevier: Amsterdam, 2013; pp. 1−42.

(2) Dang, H.-S.; Jannasch, P. Anion-Exchange Membranes with Polycationic Alkyl Side Chains Attached via Spacer Units. *J. Mater. Chem. A* **2016**, *4*, 17138−17153.

(3) Holton, O.; Stevenson, J. The Role of Platinum in Proton Exchange Membrane Fuel Cells. *Platinum Met. Rev.* **2013**, *57*, 259−271.

(4) Maurya, S.; Shin, S.-H.; Kim, Y.; Moon, S.-H. A Review on Recent Developments of Anion Exchange Membranes for Fuel Cells and Redox Flow Batteries. *RSC Adv.* **2015**, *5*, 37206−37230.

(5) Vijayakumar, V.; Nam, S. Y. Recent Advancements in Applications of Alkaline Anion Exchange Membranes for Polymer Electrolyte Fuel Cells. *J. Ind. Eng. Chem.* **2019**, *70*, 70−86.

(6) Ferriday, T. B.; Middleton, P. H. Alkaline Fuel Cell Technology - A Review. *Int. J. Hydrogen Energy* **2021**, *46*, 18489−18510.

(7) Merle, G.; Wessling, M.; Nijmeijer, K. Anion Exchange Membranes for Alkaline Fuel Cells: A Review. *J. Membr. Sci.* **2011**, *377*, 1−35.

(8) Arges, C. G.; Zhang, L. Anion Exchange Membranes' Evolution toward High Hydroxide Ion Conductivity and Alkaline Resiliency. *ACS Appl. Energy Mater.* **2018**, *1*, 2991−3012.

(9) Noh, S.; Jeon, J. Y.; Adhikari, S.; Kim, Y. S.; Bae, C. Molecular Engineering of Hydroxide Conducting Polymers for Anion Exchange Membranes in Electrochemical Energy Conversion Technology. *Acc. Chem. Res.* **2019**, *52*, 2745−2755.

(10) Varcoe, J. R.; Atanassov, P.; Dekel, D. R.; Herring, A. M.; Hickner, M. A.; Kohl, P. A.; Kucernak, A. R.; Mustain, W. E.; Nijmeijer, K.; Scott, K.; Xu, T.; Zhuang, L. Anion-Exchange Membranes in Electrochemical Energy Systems. *Energy Environ. Sci.* **2014**, *7*, 3135−3191.

(11) Pham, T. H.; Olsson, J. S.; Jannasch, P. Effects of the N-Alicyclic Cation and Backbone Structures on the Performance of Poly(Terphenyl)-Based Hydroxide Exchange Membranes. *J. Mater. Chem. A* **2019**, *7*, 15895−15906.

(12) Kang, D. H.; Das, G.; Yoon, H. H.; Kim, I. T. A Composite Anion Conducting Membrane Based on Quaternized Cellulose and Poly(Phenylene Oxide) for Alkaline Fuel Cell Applications. *Polymer* **2020**, *12*, 2676.

(13) Lu, Y.; Armentrout, A. A.; Li, J.; Tekinalp, H. L.; Nanda, J.; Ozcan, S. A Cellulose Nanocrystal-Based Composite Electrolyte with Superior Dimensional Stability for Alkaline Fuel Cell Membranes. *J. Mater. Chem. A Mater. Energy Sustain.* **2015**, *3*, 13350−13356.

(14) Ryu, J.; Seo, J. Y.; Choi, B. N.; Kim, W.-J.; Chung, C.-H. Quaternized Chitosan-Based Anion Exchange Membrane for Alkaline Direct Methanol Fuel Cells. *J. Ind. Eng. Chem.* **2019**, *73*, 254−259.

(15) Muhmed, S. A.; Nor, N. A. M.; Jaafar, J.; Ismail, A. F.; Othman, M. H. D.; Rahman, M. A.; Aziz, F.; Yusof, N. Emerging Chitosan and Cellulose Green Materials for Ion Exchange Membrane Fuel Cell: A Review. *Energy Ecol. Environ.* **2020**, *5*, 85−107.

(16) Sayari, N.; Sila, A.; Abdelmalek, B. E.; Abdallah, R. B.; Ellouz-Chaabouni, S.; Bougatef, A.; Balti, R. Chitin and Chitosan from the Norway Lobster By-Products: Antimicrobial and Anti-Proliferative Activities. *Int. J. Biol. Macromol.* **2016**, *87*, 163−171.

(17) Nam, C.-W.; Kim, Y.-H.; Ko, S.-W. Modification of Polyacrylonitrile (PAN) Fiber by Blending with N-(2-Hydroxy)-Propyl-3-Trimethyl-Ammonium Chitosan Chloride. *J. Appl. Polym. Sci.* **1999**, *74*, 2258−2265.

(18) Mohammadzadeh Pakdel, P.; Peighambardoust, S. J. Review on Recent Progress in Chitosan-Based Hydrogels for Wastewater Treatment Application. *Carbohydr. Polym.* **2018**, *201*, 264−279.

(19) Peers, S.; Montembault, A.; Ladavière, C. Chitosan Hydrogels for Sustained Drug Delivery. *J. Controlled Release* **2020**, *326*, 150−163.

(20) Liao, G.-M.; Yang, C.-C.; Hu, C.-C.; Pai, Y.-L.; Lue, S. J. Novel Quaternized Polyvinyl Alcohol/Quaternized Chitosan Nano-Composite as an Effective Hydroxide-Conducting Electrolyte. *J. Membr. Sci.* **2015**, *485*, 17−29.

(21) Liu, G.; Tsen, W.-C.; Jang, S.-C.; Hu, F.; Zhong, F.; Zhang, B.; Wang, J.; Liu, H.; Wang, G.; Wen, S.; Gong, C. Composite Membranes from Quaternized Chitosan Reinforced with Surface-Functionalized PVDF Electrospun Nanofibers for Alkaline Direct Methanol Fuel Cells. *J. Membr. Sci.* **2020**, *611*, No. 118242.

(22) Yang, J. M.; Fan, C.-S.; Wang, N.-C.; Chang, Y.-H. Evaluation of Membrane Preparation Method on the Performance of Alkaline Polymer Electrolyte: Comparison between Poly(Vinyl Alcohol)/Chitosan Blended Membrane and Poly(Vinyl Alcohol)/Chitosan Electrospun Nanofiber Composite Membranes. *Electrochim. Acta* **2018**, *266*, 332−340.

(23) Jang, S.-C.; Tsen, W.-C.; Chuang, F.-S.; Gong, C. Simultaneously Enhanced Hydroxide Conductivity and Mechanical Properties of Quaternized Chitosan/Functionalized Carbon Nano-

tubes Composite Anion Exchange Membranes. *Int. J. Hydrogen Energy* **2019**, *44*, 18134−18144.
(24) Jang, S.-C.; Chuang, F.-S.; Tsen, W.-C.; Kuo, T.-W. Quaternized Chitosan/Functionalized Carbon Nanotubes Composite Anion Exchange Membranes. *J. Appl. Polym. Sci.* **2019**, *136*, 47778.
(25) Gong, C.; Zhao, S.; Tsen, W.-C.; Hu, F.; Zhong, F.; Zhang, B.; Liu, H.; Zheng, G.; Qin, C.; Wen, S. Hierarchical Layered Double Hydroxide Coated Carbon Nanotube Modified Quaternized Chitosan/Polyvinyl Alcohol for Alkaline Direct Methanol Fuel Cells. *J. Power Sources* **2019**, *441*, No. 227176.
(26) Shi, B.; Li, Y.; Zhang, H.; Wu, W.; Ding, R.; Dang, J.; Wang, J. Tuning the Performance of Anion Exchange Membranes by Embedding Multifunctional Nanotubes into a Polymer Matrix. *J. Membr. Sci.* **2016**, *498*, 242−253.
(27) Wang, D.; Wang, Y.; Wan, H.; Wang, J.; Wang, L. Synthesis of Gemini Basic Ionic Liquids and Their Application in Anion Exchange Membranes. *RSC Adv.* **2018**, *8*, 10185−10196.
(28) Shi, B.; Zhang, J.; Wu, W.; Wang, J.; Huang, J. Controlling Conduction Environments of Anion Exchange Membrane by Functionalized SiO2 for Enhanced Hydroxide Conductivity. *J. Membr. Sci.* **2019**, *569*, 166−176.
(29) Wang, J. L.; Che, Q. T.; He, R. H. Positively Charged Polystyrene Blended Quaternized Chitosan for Anion Exchange Membranes. *J. Electrochem. Soc.* **2013**, *160*, F168−F174.
(30) Liu, G.; Tsen, W.-C.; Wen, S. Sulfonated Silica Coated Polyvinylidene Fluoride Electrospun Nanofiber-Based Composite Membranes for Direct Methanol Fuel Cells. *Mater. Des.* **2020**, *193*, No. 108806.
(31) Che, A.-F.; Liu, Z.-M.; Huang, X.-J.; Wang, Z.-G.; Xu, Z.-K. Chitosan-Modified Poly(Acrylonitrile-Co-Acrylic Acid) Nanofibrous Membranes for the Immobilization of Concanavalin A. *Biomacromolecules* **2008**, *9*, 3397−3403.
(32) Xu, G.-R.; Wang, J.-N.; Li, C.-J. Polyamide Nanofilm Composite Membranes (NCMs) Supported by Chitosan Coated Electrospun Nanofibrous Membranes: Preparation and Separation Performance Research. *Desalination* **2013**, *328*, 31−41.
(33) Chattopadhyay, D. P.; Inamdar, M. S. Studies on the Synthesis and Application of N,N,N-Trimethyl Chitosan Chloride (TMCHT) on Cotton Fabric. *J. Nat. Fibers* **2015**, *12*, 341−356.
(34) Zhao, S.; Tsen, W.-C.; Gong, C. 3D Nanoflower-like Layered Double Hydroxide Modified Quaternized Chitosan/Polyvinyl Alcohol Composite Anion Conductive Membranes for Fuel Cells. *Carbohydr. Polym.* **2021**, *256*, No. 117439.
(35) Shagdarova, B.; Lunkov, A.; Il'ina, A.; Varlamov, V. Investigation of the Properties of N-[(2-Hydroxy-3-Trimethylammonium) Propyl] Chloride Chitosan Derivatives. *Int. J. Biol. Macromol.* **2019**, *124*, 994−1001.
(36) Hou, J.; Liu, Y.; Ge, Q.; Yang, Z.; Wu, L.; Xu, T. Recyclable Cross-Linked Anion Exchange Membrane for Alkaline Fuel Cell Application. *J. Power Sources* **2018**, *375*, 404−411.
(37) Ruihua, H.; Bingchao, Y.; Zheng, D.; Wang, B. Preparation and Characterization of a Quaternized Chitosan. *J. Mater. Sci.* **2012**, *47*, 845.
(38) Akakuru, O.; Isiuku, B. Chitosan Hydrogels and Their Glutaraldehyde-Crosslinked Counterparts as Potential Drug Release and Tissue Engineering Systems - Synthesis, Characterization, Swelling Kinetics and Mechanism. *J. Phys. Chem. Biophys.* **2017**, *7*, 1−7.
(39) Karibayev, M.; Myrzakhmetov, B.; Kalybekkyzy, S.; Wang, Y.; Mentbayeva, A. Binding and Degradation Reaction of Hydroxide Ions with Several Quaternary Ammonium Head Groups of Anion Exchange Membranes Investigated by the DFT Method. *Molecules* **2022**, *27*, 2686.
(40) Rwei, S.-P.; Chen, Y.-M.; Lin, W.-Y.; Chiang, W.-Y. Synthesis and Rheological Characterization of Water-Soluble Glycidyltrimethylammonium-Chitosan. *Mar. Drugs* **2014**, *12*, 5547.
(41) Wang, L.-L.; Wang, J.-L.; Zhang, Y.; Feng, R. Alkaline Hybrid Composite Membrane for Direct Methanol Fuel Cells Application. *J. Electroanal. Chem.* **2015**, *759*, 174−183.
(42) Wu, J.; Su, Z.-G.; Ma, G.-H. A Thermo- and PH-Sensitive Hydrogel Composed of Quaternized Chitosan/Glycerophosphate. *Int. J. Pharm.* **2006**, *315*, 1−11.
(43) Stefan, J.; Lorkowska-Zawicka, B.; Kaminski, K.; Szczubialka, K.; Nowakowska, M.; Korbut, R. The Current View on Biological Potency of Cationically Modified Chitosan. *J. Physiol. Pharmacol.* **2014**, *65*, 341−347.
(44) Seong, H.-S.; Whang, H. S.; Ko, S.-W. Synthesis of a Quaternary Ammonium Derivative of Chito-Oligosaccharide as Antimicrobial Agent for Cellulosic Fibers. *J. Appl. Polym. Sci.* **2000**, *76*, 2009−2015.
(45) Yang, X.; Zhang, C.; Qiao, C.; Mu, X.; Li, T.; Xu, J.; Shi, L.; Zhang, D. A Simple and Convenient Method to Synthesize N-[(2-Hydroxyl)-Propyl-3-Trimethylammonium] Chitosan Chloride in an Ionic Liquid. *Carbohydr. Polym.* **2015**, *130*, 325−332.
(46) Freitas, E. D.; Moura, C. F., Jr.; Kerwald, J.; Beppu, M. M. An Overview of Current Knowledge on the Properties, Synthesis and Applications of Quaternary Chitosan Derivatives. *Polymers* **2020**, *12*, 2878.
(47) Wan, Y.; Creber, K. A. M.; Peppley, B.; Bui, V. T. Synthesis, Characterization and Ionic Conductive Properties of Phosphorylated Chitosan Membranes. *Macromol. Chem. Phys.* **2003**, *204*, 850−858.
(48) Mivehi, L.; Hajir Bahrami, S.; Malek, R. M. A. Properties of Polyacrylonitrile-N-(2-Hydroxy) Propyl-3-Trimethylammonium Chitosan Chloride Blend Films and Fibers. *J. Appl. Polym. Sci.* **2008**, *109*, 545−554.
(49) Wan, Y.; Peppley, B.; Creber, K. A. M.; Bui, V. T.; Halliop, E. Quaternized-Chitosan Membranes for Possible Applications in Alkaline Fuel Cells. *J. Power Sources* **2008**, *185*, 183−187.
(50) Lim, S.-H.; Hudson, S. M. Synthesis and Antimicrobial Activity of a Water-Soluble Chitosan Derivative with a Fiber-Reactive Group. *Carbohydr. Res.* **2004**, *339*, 313−319.
(51) Kulkarni, V. H.; Kulkarni, P. V.; Keshavayya, J. Glutaraldehyde-Crosslinked Chitosan Beads for Controlled Release of Diclofenac Sodium. *J. Appl. Polym. Sci.* **2007**, *103*, 211−217.
(52) Nhung, L. T.; Kim, I. Y.; Yoon, Y. S. Quaternized Chitosan-Based Anion Exchange Membrane Composited with Quaternized Poly(Vinylbenzyl Chloride)/Polysulfone Blend. *Polymers* **2020**, *12*, 2714.
(53) Wan, Y.; Peppley, B.; Creber, K. A. M.; Bui, V. T. Anion-Exchange Membranes Composed of Quaternized-Chitosan Derivatives for Alkaline Fuel Cells. *J. Power Sources* **2010**, *195*, 3785−3793.
(54) Sharma, P. P.; Jeon, Y.; Kim, D. Alkaline Stable Anion Exchange Membranes Based on Cross-Linked Poly(Arylene Ether Sulfone) Bearing Dual Quaternary Piperidines for Enhanced Anion Conductivity at Low Water Uptake. *Molecules* **2022**, *27*, 364.
(55) Frick, J. M.; Ambrosi, A.; Pollo, L. D.; Tessaro, I. C. Influence of Glutaraldehyde Crosslinking and Alkaline Post-Treatment on the Properties of Chitosan-Based Films. *J. Polym. Environ.* **2018**, *26*, 2748−2757.
(56) Badawy, S. M.; Dessouki, A. M. Cross-Linked Polyacrylonitrile Prepared by Radiation-Induced Polymerization Technique. *J. Phys. Chem. B* **2003**, *107*, 11273−11279.
(57) Liu, H.; Luo, Q.; Zhang, S.; Shi, L.; Yang, J.; Liu, R.; Wang, M.; Zhu, C.; Xu, J. New Comonomer for Polyacrylonitrile-Based Carbon Fiber: Density Functional Theory Study and Experimental Analysis. *Polymers* **2018**, *153*, 369−377.
(58) Makaremi, M.; Lim, C. X.; Pasbakhsh, P.; Lee, S. M.; Goh, K. L.; Chang, H.; Chan, E. S. Electrospun Functionalized Polyacrylonitrile−Chitosan Bi-Layer Membranes for Water Filtration Applications. *RSC Adv.* **2016**, *6*, 53882−53893.
(59) Şanli, O. Homogeneous Hydrolysis of Polyacrylonitrile by Potassium Hydroxide. *Eur. Polym. J.* **1990**, *26*, 9−13.
(60) Hu, Y.; Tsen, W.-C.; Chuang, F.-S.; Jang, S.-C.; Zhang, B.; Zheng, G.; Wen, S.; Liu, H.; Qin, C.; Gong, C. Glycine Betaine Intercalated Layered Double Hydroxide Modified Quaternized Chitosan/Polyvinyl Alcohol Composite Membranes for Alkaline Direct Methanol Fuel Cells. *Carbohydr. Polym.* **2019**, *213*, 320−328.

https://doi.org/10.1021/acsomega.2c05961
ACS Omega 2022, 7, 45371−45380

(61) Jin, S. Y.; Kim, M. H.; Jeong, Y. G.; Yoon, Y. I.; Park, W. H. Effect of alkaline hydrolysis on cyclization reaction of PAN nanofibers. *Mater. Des.* **2017**, *124*, 69−77.

https://doi.org/10.1021/acsomega.2c05961
ACS Omega 2022, 7, 45371−45380